Thermal convection in a tilted porous layer

Jan Erik Weber

Department of Mechanics

University of Oslo

Abstract.

Buoyancy-driven convection in a differentially heated, sloping porous layer is studied theoretically. For small tilt angles, a linear analysis determines the critical Rayleigh number for an infinite layer. It is shown that the preferred mode of disturbance is stationary, being longitudinal rolls with axes aligned in the direction of the basic flow. A necessary condition for instability at arbitrary tilt angles is also derived. Applying the non-linear analysis in [11] to the longitudinal roll regime, the result for the Nusselt number is found to agree well with experiment. For a vertical model of finite extent, a boundary-layer analysis is performed. Satisfactory agreement with experiment is obtained for the interior temperature distribution and the Nusselt number. The applied method also includes some effects of a variable viscosity . This is shown to introduce asymmetry into the solutions.

Nomenclature.

L, thickness of model;

H, height of model;

d, characteristic grain diameter;

k, permeability of porous medium;

g, acceleration of gravity;

c_p, specific heat at constant temperature;

x_*, y_*, z_*, Cartesian coordinates;

t_*, time;

$\vec{v}_*(= u_*, v_*, w_*)$, velocity vector;

p_*, pressure;

T_*, temperature;

ΔT, dimensional temperature difference between lower and upper plane;

W, dimensionless basic flow velocity;

$\bar{W}$, defined by (3.3);

l, m, dimensionless wave numbers in the y_*/L- and z_*/L-directions, respectively;

l_o, m_o, defined by (3.4);

c, dimensionless wave speed;

$f^{\pm}$ $(= \nu^{\pm}/\nu_r)$, defined by (6.8);

T_o, dimensionless temperature in the core;

a, defined by (8.9);

s, q, defined by (8.20) and (8.21), respectively;

∇^2, Laplacian operator;

Re, Reynolds number

Pr, Prandtl number ν_r/κ_m;

Ra, Rayleigh number $kg\gamma\Delta TL/\kappa_m\nu_r$;

R_a^*, R_o^*, R_{os}^*, defined by (3.3), (4.2) and (4.3), respectively;

Nu, Nusselt number;

C_1, C_2, defined by (8.34) and (8.35), respectively.

Greek letters.

α, dimensionless overall wave number;

β, dimensionless temperature gradient;

γ, coefficient of volume expansion;

δ, defined by (6.6);

ε, defined by (4.2);

η, defined by (8.1);

θ, Θ, dimensionless temperatures;

κ_m, thermal diffusivity;

$\vec{\lambda}$, vertical unit vector;

λ, defined by (8.11);

ν, kinematic viscosity;

ν_r, reference viscosity;

ν_1, ν_2, viscosities at the hot and cold wall, respectively;

ξ, defined by (8.18)

ρ, density;

ρ_r, reference density;

σ, dimensionless amplification factor of disturbance;

φ, tilt angle with respect to the horizontal;

ψ_*, stream function;

ψ_o, dimensionless stream function in the core;

Ω, defined by (5.3) .

Subscripts.

*, dimensional quantities;

f, fluid;

m, solid-fluid mixture;

A, average values;

Superscripts.

^, perturbation quantities;

', derivation with respect to z_*/H ;

+ - , denotes left- and right-hand boundary layer, respectively;

r, real part;

i, imaginary part.

1. Introduction.

This paper is concerned with free, thermal convection in a porous layer being tilted with respect to the horizontal. The layer is bounded by two impermeable perfectly conducting planes maintained at different temperatures, and laterally by rigid, insulating walls.

Owing to the many geophysical and technical aspects of this type of flow, convection in a horizontal layer uniformly heated from below has been studied extensively for several years. Concerning sloping porous layers, however, published works are not numerous. Most recently Bories and Combarnous [1] have studied this problem. For a vertical porous layer, we further mention the works of Schneider [2], Gill [3], Chan, Ivey and Barry [4] and Klarsfeld [5]. Due to the similarity between convection in a fluid with infinite Prandtl number and porous convection, qualitative comparisons can be made with studies on inclined and vertical fluid layers, especially those by Elder [6], Gill [7], Liang and Acrivos [8] and Hart [9].

For a tilted porous layer, the main experimental results are as follows. At small Rayleigh numbers the motion is unicellular, constituting a basic flow. When the Rayleigh number, or the tilt angle, are sufficiently increased, instability occurs as two-dimensional disturbances with axes aligned in the direction of the basic flow (longitudinal rolls). When the tilt angle approaches 90°, the disturbances tend to zero. At sufficiently high Rayleigh numbers, the basic flow in a vertical layer exhibits boundary layer character. Distinct thermal boundary layers develop along

the vertical walls, while the core-region is characterized by a positive vertical temperature gradient.

In the present paper we study both the longitudinal roll regime in a tilted layer and the boundary-layer flow in a vertical model. The method applied in the latter investigation is similar to that developed by Gill [7] for the analogous fluid problem. In the present study the method is extended to include some effects of a variable kinematic viscosity. This is motivated by the fact that ν in practice may vary considerably due to the large values of ΔT often involved in this type of flow.

2. Governing equations.

Consider natural three-dimensional convection in an enclosed porous medium with rectangular, impermeable boundaries. The layer is tilted an angle φ with respect to the horizontal, and L and H are the thickness and the height, respectively, of the model (figure 1). The width, in the y_*-direction, is infinite. The lower and upper planes are taken to be perfect heat conductors and maintained at the temperatures $\Delta T/2$ and $-\Delta T/2$, respectively, while the lateral boundaries are insulating.

Making the Bousinesq approximation, the equations of motion, heat and continuity can be stated as follows, respectively,

$$\frac{1}{\rho_r} \nabla p_* + \frac{\nu}{k} \vec{v}_* - g\gamma T_* \vec{\lambda} = 0 \qquad (2.1)$$

$$\frac{(c_p\rho)_m}{(c_p\rho)_f} \frac{\partial T_*}{\partial t_*} + \vec{v}_* \cdot \nabla T_* = \kappa_m \nabla^2 T_* \qquad (2.2)$$

$$\nabla \cdot \vec{v}_* = 0 \qquad (2.3)$$

where $\vec{\lambda} = (\cos\varphi, 0, \sin\varphi)$ is the vertical unit vector. In this part of the analysis we take the kinematic viscosity to be constant, $\nu = \nu_r$. Dimensionless variables may then be introduced by choosing

$$L,\ (c_p\rho)_m L^2/(c_p\rho)_f \kappa_m,\ \kappa_m/L,\ \Delta T,\ \rho_r \nu_r \kappa_m/k \tag{2.4}$$

as units of length, time, velocity, temperature and pressure, respectively. The governing equations can now be written

$$\begin{aligned} \nabla p + \vec{v} - Ra\, T\vec{\lambda} &= 0 \\ \frac{\partial T}{\partial t} + \vec{v}\cdot\nabla T &= \nabla^2 T \\ \nabla\cdot\vec{v} &= 0 \end{aligned} \tag{2.5}$$

where unmarked quantities are non-dimensional.
As shown in [1] this system permits a particular steady solution when the effect of the lateral end-walls can be neglected, i.e. when $L/H \approx 0$. Taking

$$\begin{aligned} &\partial/\partial t = \partial/\partial y = \partial/\partial z = u = v = 0 \\ &w = W(x), \quad T = \Theta(x) \end{aligned} \tag{2.6}$$

where $\Theta(\pm\frac{1}{2}) = \mp\frac{1}{2}$, it is easily found from (2.5) that

$$\begin{aligned} W(x) &= -Ra \sin\varphi\, x \\ \Theta(x) &= -x \end{aligned} \tag{2.7}$$

Perturbating this solution with respect to arbitrary disturbances (denoted by carets), the resulting velocity and temperature fields may be written

$$\begin{aligned} u,v,w &= (\hat{u},\hat{v},W(x) + \hat{w}) \\ T &= \Theta(x) + \hat{\theta} \end{aligned} \tag{2.8}$$

Introducing this into (2.5), and eliminating the pressure , we finally obtain

$$\nabla^2 u - Ra\cos\varphi \nabla_1^2 \theta + Ra \sin\varphi \theta_{xz} = 0 \qquad (2.10)$$

$$\theta_t - u + W(x)\theta_z + \vec{v}\cdot\nabla\theta = \nabla^2\theta \qquad (2.11)$$

where $\nabla_1^2 = \partial^2/\partial y^2 + \partial^2/\partial z^2$, and the carets have been dropped. The boundary conditions are $u = \theta = 0$ for $x = \pm \frac{1}{2}$

3. Linear stability analysis for an infinite layer.

Consider infinitesimal disturbances. Then the non-linear term in (2.11) can be neglected. Let

$$u,v,w,\theta = \{u(x),v(x),w(x),\theta(x)\}\exp(i(ly + mz) + \sigma t) \qquad (3.1)$$

where l and m are real wave numbers in the y- and z-direction, respectively, and σ the complex growth rate. By eliminating u between (2.10) and (2.11), we finally obtain

$$(D^2-\alpha^2)^2\theta - \sigma(D^2-\alpha^2)\theta - \alpha^2 Ra^*\theta - imRa^* tg\varphi[\bar{W}(D^2-\alpha^2)\theta - D\theta] = 0 \qquad (3.2)$$

to be solved subject to $\theta = D^2\theta = 0$ for $x = \pm \frac{1}{2}$.

Here
$$D = \frac{d}{dx}, \quad Ra^* = Ra\cos\varphi, \quad \alpha^2 = l^2+m^2 \qquad (3.3)$$
and
$$\bar{W} = W/Ra\sin\varphi = -x$$

When φ is small, this system can be solved by expanding the variables after $tg\varphi$ as a small parameter. However, equation (3.2) is nearly similar to that treated by Weber [10] (equation 3.10),

except for a different sign in the last term and one additional term proportional to the square of the small parameter.

Accordingly the results for the present stability problem can be derived from the analysis in [10]. For the tilted porous layer problem we then obtain, (i) the principle of exchange of stabilities is valid when φ is small, (ii) the critical Rayleigh number can be written

$$Ra^* = Ra \cos\varphi = 4\pi^2 + 3m_0^2 tg^2\varphi + O(tg^4\varphi) \tag{3.4}$$

where

$$l_0^2 + m_0^2 = \pi^2$$

Here the subscript 0 refers to the first term in a series expansion after $tg\varphi$. For a purely two-dimensional disturbance with axis normal to the basic flow (a transverse roll) $l_0 = 0$, while for a longitudinal roll $m_0 = 0$. Accordingly longitudinal rolls minimize the Rayleigh number, and will therefore constitute the preferred mode. This result is analogous to that of Liang and Acrivos [8] for a tilted fluid layer. The occurrence of longitudinal rolls with wave number π, and a critical Rayleigh number given by $Ra \cos\varphi = 4\pi^2$ have been confirmed experimentally by Bories and Combarnous [1]. They also showed that longitudinal rolls constituted a possible stationary solution of the linearized problem.

For a nearly vertical layer, observations show that the basic solution is stable. This can also be demonstrated analytically. Multiplying (3.2) by the complex conjugate of θ, and integrating from $x = -\frac{1}{2}$ to $x = \frac{1}{2}$, we obtain from the real and imaginary

parts, respectively, that

$$\sigma^r<|D\theta|^2+\alpha^2|\theta|> = - <|D^2\theta|^2+2\alpha^2|D\theta|^2+\alpha^4|\theta|^2> + \alpha^2 Ra\cos\varphi<|\theta|^2> \quad (3.5)$$

$$\sigma^i<|D\theta|^2+\alpha^2|\theta|^2>= - m\,Ra\sin\varphi<\overline{W}(|D\theta|^2+\alpha^2|\theta|^2)> \quad (3.6)$$

Here the brackets denote integration from $x = -\frac{1}{2}$ to $x = +\frac{1}{2}$.

For a disturbance to grow, σ^r in (3.5) must be positive. Hence we obtain as a necessary condition for instability that

$$Ra \cos \varphi > 0 \quad (3.7)$$

For $\varphi = 90^\circ$ then, the basic flow is stable, as shown by Gill [3]. This will also be the case for $90^\circ \leq \varphi \leq 180^\circ$ (heating from above). The stability of flow in a vertical porous layer is attributed to the lack of inertial terms in the equation of motion (thereby inhibiting shear-instability).

From (3.6) we note that an unstable longitudinal roll always is stationary. For a transverse roll the wave speed c is given by $c = \sigma^i/m$. From (3.6) we then obtain the result that

$$|c| < \tfrac{1}{2} Ra \sin \varphi = W_{max} \quad (3.8)$$

When $\sin \varphi = 0$, we observe that the principle of exchange of stabilities is valid (which of course is well known).

4. Non-linear analysis of longitudinal rolls.

As confirmed experimentally in [1], the longitudinal roll solution exhibits no z-dependence for moderate values of the Rayleigh number and the tilt angle. Accordingly we may take $\partial/\partial z = 0$ and

and look for a stationary solution of the non-linear system (2.10) - (2.11). The equations reduce to

$$\begin{aligned} u_{xx} + u_{yy} &= Ra \cos\varphi\, \theta_{yy} \\ \theta_{xx} + \theta_{yy} + u &= u\theta_x + v\theta_y \\ u_x + v_y &= 0 \end{aligned} \tag{4.1}$$

This system is identical to that governing two-dimensional convection in a horizontal porous layer, except that the acceleration of gravity is diminished by the factor $\cos\varphi$. Hence the analysis of Palm, Weber and Kvernvold [11] can be applied directly to this problem, substituting $g\cos\varphi$ for g. Only the result for the Nusselt number will be given here.

Defining

$$\varepsilon^2 = (Ra^* - R_0^*)/Ra^* \tag{4.2}$$

where $Ra^* = Ra \cos\varphi$ and $R_0^* = 4\pi^2$, the Nusselt number to sixth order may be written

$$\begin{aligned} Nu = 1 &+ 2\left(\frac{R_{os}^*}{R_o^*}\right)\varepsilon^2 + 2\,\frac{R_{os}^*}{R_o^*}\left(1 - \frac{17}{24}\,\frac{R_{os}^*}{R_o^*}\right)\varepsilon^4 \\ &+ 2\,\frac{R_{os}^*}{R_o^*}\left(1 - \frac{17}{12}\,\frac{R_{os}^*}{R_o^*} + \frac{191}{288}\left(\frac{R_{os}^*}{R_o^*}\right)^2\right)\varepsilon^6 . \end{aligned} \tag{4.3}$$

Here $R_{os}^* = R_o^*/(1-\varepsilon^{2s})$, and in this approximation, $s = 3$.

In figure 2 this result is compared with the experiments and the theoretical analysis by Bories and Combarnous [1]. We emphasize

that (4.3) is valid for Ra and φ such that effects due to the end-walls can be neglected. For the experiments in [1] where L/H = 0.075, this is shown to hold when $\varphi \lesssim 50^{\circ}$ and Ra < 250.

Actually hexagones were observed in [1] for tilt angles less than about 15°, while longitudinal rolls took over for $\varphi \gtrsim 15^{\circ}$. The preference of hexagones in a nearly horizontal layer, however, may be attributed to non-linear effects such as variation of ν and κ_m with temperature (Palm [12], Busse [13]) or time dependent boundary conditions (Krishnamurti [14]).

5. Vertical layer of finite extent.

For larger values of Ra and φ the end-walls can no longer be neglected. Due to their presence, a stable vertical temperature gradient will develop in the interior of the layer. Consider a vertical layer. According to the remarks above, we now assume a solution of the form

$$W = W(x)$$
$$T = \Theta(x) + \beta z \qquad (5.1)$$

where $\beta > 0$. Here, as before, $\Theta(\pm \tfrac{1}{2}) = \mp \tfrac{1}{2}$. Further, the conservation of mass leads to

$$\int_{-\frac{1}{2}}^{+\frac{1}{2}} W(x)dx = 0 \qquad (5.2)$$

From (2.5) we then obtain

$$W = -\frac{Ra}{2}\frac{\sinh(\Omega x)}{\sinh(\Omega/2)}$$

$$T = -\tfrac{1}{2}\frac{\sinh(\Omega x)}{\sinh(\Omega/2)} + \beta z \qquad (5.3)$$

where $\Omega^2 = \beta Ra$.

This is of course only an exact solution of the problem if $T = \pm\tfrac{1}{2} + \beta z$ at the two vertical boundaries. However, it is assumed that (5.3) is a good approximation to what actually occurs in the central part of the layer when L/H is small. For a fluid slot, this assumption has been confirmed experimentally ([6],[9]). The value of β will vary with Ra. Introducing a dimensional temperature gradient β_* by

$$\beta = \frac{\beta_*}{\Delta T/H}\left(\frac{L}{H}\right) , \qquad (5.4)$$

it is shown for a vertical fluid slot that β_* assumes an asymptotic value of roughly $\Delta T/2H$.

From (5.3) the Nusselt number may be written

$$Nu = -(D\Theta)_{X=-\frac{1}{2}} = \tfrac{1}{2}\Omega\coth(\Omega/2) \qquad (5.5)$$

When Ω is sufficiently large, this reduces to

$$Nu = \tfrac{1}{2}\Omega . \qquad (5.6)$$

Taking $\beta = \text{const} \times L/H$, we obtain from (5.6)

$$Nu = C\left(\frac{L}{H}\right)^{\frac{1}{2}} Ra^{\frac{1}{2}} \qquad (5.7)$$

where C is a dimensionless constant. A similar formula is given in [5]. (5.7) may also be derived by a simple order of magnitude analysis.

To determine analytically the temperature distribution in the interior of the layer, a two-dimensional analysis must be performed. This is done in the next section in the limit of large Rayleigh numbers.

6. Boundary-layer analysis for a vertical layer.

As confirmed experimentally in [1] and [5], thermal boundary layers develop along the vertical walls, when Ra is large. Accordingly we may perform a boundary-layer analysis of the problem. For two-dimensional flow we obtain from (2.1) and (2.2)

$$\frac{\partial}{\partial x_*}(\nu w_*) - \frac{\partial}{\partial z_*}(\nu u_*) = kg\gamma \frac{\partial T_*}{\partial x_*} \tag{6.1}$$

$$u_* \frac{\partial T_*}{\partial x_*} + w_* \frac{\partial T_*}{\partial z_*} = \kappa_m \left(\frac{\partial^2 T_*}{\partial x_*^2} + \frac{\partial^2 T_*}{\partial z_*^2}\right) \tag{6.2}$$

where we have allowed for a variable viscosity in (6.1). This is relevant, since in practice the viscosity may vary rapidly with temperature.

The continuity equation now implies the existence of a stream function ψ_* such that

$$u_* = -\frac{\partial \psi_*}{\partial z_*} , \qquad w_* = \frac{\partial \psi_*}{\partial x_*} \tag{6.3}$$

Accordingly the boundary conditions may be stated as

$$\begin{aligned} &\psi_* = 0 , \quad T_* = \mp \tfrac{1}{2} \Delta T \quad \text{on} \quad x_* = \pm \tfrac{1}{2} L \\ &\psi_* = 0 , \quad \frac{\partial T_*}{\partial z_*} = 0 \quad \text{on} \quad z_* = \pm \tfrac{1}{2} H \end{aligned} \tag{6.4}$$

The thickness of the boundary layers on the vertical walls is taken to be of order δ. We assume that δ is small compared to both L and H, so the boundary layers on the two walls are distinct and separated by a core region. The vertical length scale is assumed to be of order H. Since the temperature variation over the vertical boundary layers must be of order ΔT, balance between convection and conduction in the heat equation requires that

$$\psi_* \sim \kappa_m H/\delta \tag{6.5}$$

where $\sim$ means of the order of.

From (5.1) a balance between buoyancy and vorticity yields

$$\delta^2 \sim \frac{H\nu_r\kappa_m}{kg\gamma\Delta T} \tag{6.6}$$

where ν_r is a reference viscosity.

We now introduce non-dimensional quantities by taking $\delta = (H\nu_r\kappa_m/kg\gamma\Delta T)^{\frac{1}{2}}$ as horizontal length scale and defining new variables by

$$x^{\pm} = (L/2 \pm x_*)/\delta \ , \qquad z = z_*/H \ , \qquad T = T_*/\Delta T \tag{6.7}$$

and

$$\psi = \psi_*/(\kappa_m H/\delta) \ .$$

Here the plus and minus signs in the definition of the horizontal coordinate correspond to the left- and right-hand boundary layers, respectively (this sign convention will be adopted for the rest of the analysis, if nothing else is stated).

The approximate forms of (6.1) - (6.3) valid in the boundary layers may then be written

$$(f^{\pm}w)_x = T_x \tag{6.8}$$

$$\pm uT_x + wT_z = T_{xx} \tag{6.9}$$

$$u = -\psi_z , \quad w = \pm\psi_x \tag{6.10}$$

where

$$f^{\pm} = \nu^{\pm}/\nu_r .$$

In (6.8)-(6.10) a $\pm$ superscript should be understood in the x-coordinate, but it is not stated for the reason of simplicity. By the definitions (6.7), $x^{\pm}$ is always positive, belonging to the interval $[0,\infty>$, while $-\frac{1}{2} \leq z \leq +\frac{1}{2}$.

On the vertical walls we have $\psi = 0$ and $T = \pm\frac{1}{2}$. When $z \to \pm\frac{1}{2}$ the solutions must match solutions valid in the corners, and when $x \to \infty$ the solutions must match a solution valid in the core.

7. The core solution.

Consider the solutions in the core. We assume that the scales of the stream function, temperature and vertical distance are the same as those in the boundary layers, while the characteristic horizontal length is taken to be L. In (6.1) the vorticity terms are respectively of order δ/L and $\delta L/H^2$ compared with the buoyancy term. These orders of magnitude are both small compared with unity provided

$$\delta \ll L \quad \text{and} \quad \delta \ll H^2/L \tag{7.1}$$

As required earlier, $\delta << L$ and $\delta << H$ to assure distinct boundary layers. (7.1) is clearly satisfied then, if $H \geq L$, which is the case of interest in this problem. Utilizing (7.1), equation (6.1) in the core reduces to

$$T_x = 0 \tag{7.2}$$

as a first approximation. Hence

$$T = T_o(z) \tag{7.3}$$

in the core.

In (6.2) the conduction terms are respectively of order δ/L and $\delta L/H^2$ compared with the convection terms. If now (7.1) is satisfied, the heat equation in the core reduces to

$$\psi_x T_o' = 0 \tag{7.4}$$

where we have utilized that $T_x = 0$ from (7.2), and the prime denotes derivation with respect to z. Since by experimental evidence, $T_o' \neq 0$ in the central part of the layer, (7.4) implies that

$$\psi = \psi_o(z) \tag{7.5}$$

in the core. Accordingly, to this approximation, the vertical velocity in the core is zero. Further T, ψ must tend to T_o, ψ_o as $x \to \infty$.

8. Approximate solution of the boundary-layer equations.

Utilizing (7.3) and (7.5), we define

$$T = T_o(z) + \theta(x,z)$$
$$\psi = \psi_o(z) + \eta(x,z) \qquad (8.1)$$

where θ and η satisfy

$$\theta, \eta \to 0 \quad \text{as} \quad x \to \infty \qquad (8.2)$$

Equation (6.8) may be integrated directly. By the aid of (8.1), the system of equations is written

$$f^{\pm} w = \theta \qquad (8.3)$$

$$\pm u \theta_x + w T_z = \theta_{xx} \qquad (8.4)$$

$$u = - \psi_o' - \eta_z , \qquad w = \pm \eta_x \qquad (8.5)$$

where, as adopted, the plus and minus signs correspond to the left- and right-hand boundary layers, respectively.

Analogous to Gill [7], the nonlinear system (8.3) - (8.5) will be solved by a modified Oseen technique. Since u and T_z in (8.4) at each level z = const. varies across the boundary layers from zero on the vertical walls to $u_o(z)$ and $T_o'(z)$ in the core, they may as an approximation be replaced at each level by average values $u_A(z)$ and $T_A'(z)$ which must be the same in both boundary layers. Also f in (8.3) will be replaced at each level by an average value $f_A = f(T_A)$. With these assumptions, the vorticity and heat equations may be written

$$f_A^{\pm} w = \theta \tag{8.6}$$

$$\pm u_A \theta_x + w T_A' = \theta_{xx} , \tag{8.7}$$

or, by eliminating w from (8.7)

$$\theta_{xx} - (\pm u_A)\theta_x - (T_A'/f_A^{\pm})\theta = 0 \tag{8.8}$$

Here the coefficients are independent of x. Accordingly the solution may be written

$$\theta \propto a(z) e^{-\lambda(z)x} \tag{8.9}$$

where λ is given by

$$\lambda^2 + (\pm u_A)\lambda - T_A'/f_A^{\pm} = 0 \tag{8.10}$$

As mentioned before, experiments show that the temperature gradient in the core is positive. Hence we concentrate about the case where $T_A' > 0$. This means from (8.10) that λ is always real. Further λ must be positive to satisfy the requirement that $\theta \to 0$ as $x \to \infty$. Hence, from (8.10)

$$\lambda = -\tfrac{1}{2}(\pm u_A) + \tfrac{1}{2}\sqrt{u_A^2 + 4T_A'/f_A^{\pm}} \tag{8.11}$$

Applying the boundary conditions at $x = 0$, we obtain from (8.1) and (8.9) that $a(z) = \pm\tfrac{1}{2} - T_o$. The temperature and the vertical velocity in the boundary layers may then be written

$$\theta = T - T_o = (\pm\tfrac{1}{2} - T_o)e^{-\lambda x} \tag{8.12}$$

$$w = \frac{(\pm\frac{1}{2} - T_o)e^{-\lambda x}}{f_A^{\pm}} \tag{8.13}$$

To relate u_A and T'_A to the core values u_o, T'_o, we apply integral conditions obtained by integrating the continuity and heat equations, (8.5) and (8.4), across each boundary layer. This leads to

$$\int_o^\infty w\,dx = \pm\,\psi_o \tag{8.14}$$

$$\frac{d}{dz}\int_o^\infty w\,\theta\,dx \pm T'_o\psi_o = -\,(\theta_x)_{x=0} \tag{8.15}$$

Momentum is conserved automatically since (8.3) is satisfied exactly. Inserting from (8.12) and (8.13) into these equations, we finally obtain

$$\pm\,\psi_o = \frac{\pm\frac{1}{2}-T_o}{\lambda f_A^{\pm}} \tag{8.16}$$

$$\frac{d}{dz}(\lambda f_A^{\pm}) = -\,\frac{2\lambda^3(f_A^{\pm})^2}{\pm\frac{1}{2}-T_o} \tag{8.17}$$

where λ is given by (8.11)

To solve (8.16) - (8.17) we must assume a relation between the temperature and the viscosity. When the temperature varies considerably, it is not possible to derive any simple general relationship between T_* and ν. To retain some general effects of a variable viscosity, and still have a tractable mathematical problem, we have to make some simplifying assumptions. Accordingly we take the viscosity to vary linearly over the boundary layers, and to be independent of height. If ν_1 and ν_2 are the viscosities at the hot and cold wall, resepctively, and $\nu_r = (\nu_1+\nu_2)/2$ is the mean viscosity, we obtain

$$f_A^+ = \nu_A^+/\nu_r = 1 - \xi$$

$$f_A^- = \nu_A^-/\nu_r = 1 + \xi \qquad (8.18)$$

where

$$\xi = \tfrac{1}{2}\,\frac{\nu_2-\nu_1}{\nu_2+\nu_1}$$

For most liquids ξ is positive, while for most gases it is negative.

Relation (8.11) can be stated explicitly as

$$\lambda^+ = -\tfrac{1}{2}\,u_A + \tfrac{1}{2}\sqrt{u_A^2 + 4T_A'/(1-\xi)}$$

$$\lambda^- = +\tfrac{1}{2}\,u_A + \tfrac{1}{2}\sqrt{u_A^2 + 4T_A'/(1+\xi)} \qquad (8.19)$$

Suitable new variables may be introduced by taking

$$s = \lambda^+ + \lambda^- \qquad (8.20)$$

$$q = (\lambda^- - \lambda^+)/s \qquad (8.21)$$

Equations (8.16), (8.17) then yield

$$\psi_o = \frac{\frac{1}{2} - T_o}{\lambda^+(1-\xi)} \qquad (8.22)$$

$$\psi_o = \frac{\frac{1}{2} + T_o}{\lambda^-(1+\xi)} \qquad (8.23)$$

$$\frac{d}{dz}(\lambda^+) = -\frac{2(\lambda^+)^3(1-\xi)}{\frac{1}{2} - T_o} \qquad (8.24)$$

$$\frac{d}{dz}(\lambda^-) = \frac{2(\lambda^-)^3(1+\xi)}{\frac{1}{2} + T_o} \qquad (8.25)$$

From (8.22) and (8.23) we readily obtain

$$T_o = \tfrac{1}{2}\,\frac{q+\xi}{1+\xi q} \tag{8.26}$$

$$\psi_o = \frac{1}{s(1+\xi q)} \tag{8.27}$$

while (8.24) and (8.25) reduce to

$$\frac{ds}{dz} = 2s^3 q(1+\xi q) \tag{8.28}$$

$$\frac{d}{dz}(sq) = s^3(1+q^2)(1+\xi q) \tag{8.29}$$

By eliminating dz, the relation between s and q can be integrated immediately, giving

$$s = \frac{1}{C_1(1-q^2)} \tag{8.30}$$

where C_1 is a constant. Hence, from (8.27)

$$\psi_o = C_1\,\frac{(1-q^2)}{(1+\xi q)} \tag{8.31}$$

Now, combining (8.28) and (8.30), we obtain a relationship between q and z. It is

$$\frac{z}{C_1^2} = \frac{1}{\xi}\left[\frac{q}{\xi} - \tfrac{1}{2}\,q^2 - \left(\frac{1-\xi^2}{\xi^2}\right)\ln(1+\xi q)\right] + C_2 \tag{8.32}$$

The constants C_1 and C_2 should have been determined by matching with the solutions valid in the horizontal boundary layers. However, effects due to their presence are neglected in this analysis. Analogous to Gill [7] we then take the inner solution to be valid at the horizontal end-walls, i.e.

$$\psi_0 = 0 \quad \text{on} \quad z = \pm \tfrac{1}{2} \tag{8.33}$$

From (8.31) this implies that $q(z = \pm \frac{1}{2}) = \pm 1$, and hence from (8.32)

$$C_1 = \left[(\tfrac{\xi}{2}) / (\tfrac{1}{\xi} + (\tfrac{1-\xi^2}{\xi^2}) \ln(\tfrac{(1-\xi^2)^{\frac{1}{2}}}{1+\xi})) \right]^{\frac{1}{2}} \tag{8.34}$$

$$C_2 = \frac{1}{2\xi} \left[1 + (\tfrac{1-\xi^2}{\xi^2}) \ln(1-\xi^2) \right] \tag{8.35}$$

When ξ tends to zero, it easily is shown that the relations above reduce to

$$\frac{z}{C_1^2} = q - \tfrac{1}{3} q^3 \quad \text{where} \quad C_1 = \tfrac{1}{2}\sqrt{3} \quad \text{and} \quad C_2 = 0 \tag{8.36}$$

In this case the temperature gradient in the middle is given by

$$\beta = (T_0')_{z=0} = 2/3 \tag{8.37}$$

Combining (8.20), (8.21) and (8.30) we finally obtain λ as a function of q, being

$$\lambda^{\pm} = \frac{1}{2C_1(1 \pm q)} \tag{8.38}$$

Hence all quantities in the expressions for the vertical velocity and the temperature, (8.12), (8.13), now are determined as functions of q (and thereby z, via (8.32)). The results will be discussed in the next section.

Finally it should be noted that the solutions have singularities in the corners $(-\frac{1}{2}L, -\frac{1}{2}H)$ and $(\frac{1}{2}L, \frac{1}{2}H)$. This is analogous to the result in [7].

9. Results and discussion.

In figures 3-6 T_o, ψ_o etc. are shown as functions of z. For constant viscosity, $\xi = 0$, (solid lines) the solutions exhibit centro-symmetrical properties. This is in accordance with the system of equations and boundary conditions for that particular case, and has been used explicitly by Gill [7] in his method of solution. The broken lines in figures 3-6 correspond to $\xi = 0{\cdot}25$, which means that the viscosity increases by a factor 3 from the hot to the cold wall. The figures clearly show that a variable ν introduces asymmetry into the solutions, as suggested by Gill.

From figure 3 we observe that the interior temperature distribution is close to a straight line in the central part of the layer. The plotted points are experimental values taken from Klarsfeld [5] using chlorobenzéne as saturating fluid. The variation of ν is not significant in his experiment, being less than ten per cent over the layer. It is seen that the theoretical curve corresponding to constant viscosity agrees well with the experiments. For the temperature gradient β in the middle of the layer, we get the value $0{\cdot}67$ from (8.37). The experiments plotted in figure 3 gives approximately $\beta = 0{\cdot}69$. For comparison we mention that Hart [9] has measured a gradient of $0{\cdot}62$ for the similar problem in a fluid layer.

The value of the stream function ψ_o in the core is plotted in figure 4. Introducing the horizontal core velocity $u_o = -\psi_o'$, we see that most of the mass flux across the core takes place near the upper and lower boundaries. This is in accordance with the observations in [5]. At the horizontal boundaries u_o tends to infinity, and so does also the temperature gradient (figure 3). This occures because we have neglected the effect of boundary layers

at the horizontal end-walls. Taking these into account, the velocity and temperature gradient will be modified.

In figure 5 the vertical velocities w^+ and w^- at the left- and right-hand walls respectively, are plotted as functions of z. In figure 6 a similar plot is done for the boundary-layer thicknesses $1/\lambda^+$ and $1/\lambda^-$. We observe that a variable viscosity results in a higher velocity and a thinner boundary layer at the hot wall, and vice versa at the cold wall. This conforms to the observations by Elder [6] in a fluid slot. In figure 7 we have displayed the temperature variation in the left-hand boundary layer as a function of x for four different values of z. The three upper curves can only qualitatively be compared with the experimental resutls in [1] (figure 9 c), since the left-hand wall was not isothermal in this experiment.

The heat transfer across the layer may be expressed by the Nusselt number

$$Nu = \frac{1}{\Delta T\ H/L} \int_{-\frac{1}{2}H}^{+\frac{1}{2}H} -\left(\frac{\partial T_*}{\partial x_*}\right)_{x_*=-\frac{1}{2}L} dz_* \qquad (9.1)$$

which is the ratio of the total heat transport to the heat transferred by pure conduction. Taking $\xi = 0$, the integration yields

$$Nu = \frac{\sqrt{3}}{3}\left(\frac{L}{H}\right)^{\frac{1}{2}} Ra^{\frac{1}{2}} \qquad (9.2)$$

which is similar to (5.7) with $C = \frac{\sqrt{3}}{3}$. Bories and Combarnous [1] report an empirical formula for the Nusselt number in a vertical layer involving L/H (in our notation) and Ra to the powers of $0{\cdot}397$ and $0{\cdot}625$, respectively, including all their experiments.

However, only for their last run (Ra = 520) the flow exhibited boundary-layer character. Accordingly the proposed formula can not be valid in the limit of large Ra. It seems plausible then, as the Rayleigh number increases, that both exponents should tend to 0•5 as a limit.

10. Summary and concluding remarks.

According to the results presented above, instability in an infinite porous layer, being slightly tilted with respect to the horizontal, occurs when $Ra \cos \varphi = 4\pi^2$. The preferred mode of disturbance will be stationary, longitudinal rolls having axes aligned in the directed of the basic flow. The critical dimensional wave length is given by 2L. For the basic solution to become unstable, we obtain as a necessary condition that $Ra \cos \varphi > 0$. Hence the motion is stable when $90^\circ \leq \varphi \leq 180^\circ$. Concerning longitudinal rolls, it is shown that the computations in [11] may be applied directly to the present problem. The result so obtained for the Nusselt number fits well with experiment.

For a vertical layer, the effect of the horizontal end-walls are taken into account. A boundary-layer analysis is performed using a method developed by Gill [7] for the analogous problem in a fluid slot. In the present paper this method has been extended to include some effects of a variable viscosity. This is shown to introduce asymmetry into the solutions. For the interior temperature distribution and the Nusselt number, satisfactory agreement has been obtained with the experimental results in [5] and [1].

Finally it should be noted that for a boundary-layer analysis to be valid in a porous vertical layer, more conditions must be imposed than for the similar fluid flow problem. For both problems the magnitude δ of the boundary layers must be much smaller than the horizontal and vertical extent of the model. For a porous layer, this leads to

$$(\frac{H}{L})^{\frac{1}{2}} << Ra^{\frac{1}{2}} \tag{10.1}$$

since we concentrate about $H \geq L$.

To use Darcy's law in the boundary layers, we also must require that the Reynolds number defined with respect to the characteristic grain diameter, d, not exceeds unity. Defining a Reynolds number by

$$Re = \frac{d}{\nu_r}(w_*)_{x_*=-\frac{1}{2}L} \tag{10.2}$$

and substituting the value for $z_* = 0$, i.e. $w_* = \kappa_m H/2\delta^2$, the above requirement implies

$$\frac{d}{L} < 2 \, Pr \, Ra^{-1} \tag{10.3}$$

Further, to use porous media considerations in the boundary layers, the grain diameter must be smaller than the boundary-layer thickness, i.e. $d < \delta$. This leads to

$$\frac{d}{L} < (\frac{H}{L})^{\frac{1}{2}} Ra^{-\frac{1}{2}} \tag{10.4}$$

For given geometry and Rayleigh number, then, the value of Pr decides which condition (10.3), (10.4) will be the most restrictive.

REFERENCES

[1] S.A.Bories and M.A.Combarnous, Natural convection in a sloping porous layer, J.Fluid Mech. 57, 63 (1973)

[2] K.-J.Schneider, Investigation of the influence of free thermal convection on heat transfer through granular material, 11th Int.Cong.of Refrigeration, Munich Paper, no.11-4 (1963)

[3] A.E.Gill, A proof that convection in a porous vertical slab is stable, J.Fluid Mech. 35, 545 (1969)

[4] B.K.C.Chan, C.M.Ivey and J.M.Barry, Natural convection in enclosed porous media with rectangular boundaries, J.Heat Transfer 92 (1),21 (1970)

[5] S.M.Klarsfeld, Champs de temperature associés aux mouvements de convection naturelle dans un milieu poreux limité, Revue Gén.Therm. 9 (108) 1403 (1970)

[6] J.W.Elder, Laminar free convection in a vertical slot, J.Fluid Mech. 23, 77 (1965)

[7] A.E.Gill, The boundary-layer regime for convection in a rectangular cavity, J.Fluid Mech. 26, 515 (1966)

[8] S.F.Liang and A.Acrivos, Stability of buoyancy-driven convection in a tilted slot, Int.J.Heat Mass Transfer, 13, 449(1970)

[9] J.E.Hart, Stability of the flow in a differentially heated inclined box, J.Fluid Mech. 47, 547 (1971)

[10] J.E.Weber, Convection in a porous medium with horizontal and vertical temperature gradients, to appear in Int.J.Heat Mass. Transfer.

[11] E.Palm, J.E.Weber and O.Kvernvold, On steady convection in a porous medium, J.Fluid Mech. 54, 153 (1972)

[12] E.Palm, On the tendency towards hexagonal cells in steady convection, J.Fluid Mech. 8, 183 (1960)

[13] F.H.Busse, The stability of finite amplitude convection and its relation to an extremum principle, J.Fluid Mech. 30, 625 (1967).

[14] R.Krishnamurti, Finite amplitude convection with changing mean temperature. Part 1. Theory, J.Fluid Mech. 33 457, (1968)

Figure legends

Figure 1. The porous model. The y_*-axis is normal to the plane of the paper.

Figure 2. Values of Nu vs. Ra cos φ for longitudinal rolls; ——, the result (4.3) obtained from Palm, Weber and Kvernvold [11]; -•-•, limiting curves for the experimental data by Bories and Combarnous [1] for various tilt angles (0-60°); ----, result from the theoretical analysis in [1].

Figure 3. The temperature $T_0(z)$ in the core. The solid line corresponds to constant viscosity, $\xi = 0$, while the broken line is for $\xi = 0{\cdot}25$ i.e. $\nu_2 = 3\nu_1$. The experimental points are from Klarsfeld [5] (figure 11 (E10) where Ra = 1298 and H/L = 2·25). Here the variation of ν is not significant (less than 10 percent).

Figure 4. The stream function $\psi_0(z)$ for the core. Solid and broken lines correspond to $\xi = 0$ and $\xi = 0{\cdot}25$, respectively.

Figure 5. Vertical velocities at (a) the left-hand and (b) the right-hand boundaries. Solid and broken lines correspond to $\xi = 0$ and $\xi = 0{\cdot}25$, respectively.

Figure 6. Boundary layer thicknesses at (a) the left-hand and (b) the right-hand walls. Solid and broken lines correspond to $\xi = 0$ and $\xi = 0{\cdot}25$, respectively.

Figure 7. Variation with x of the temperature in the left-hand boundary layer at four different levels of height.

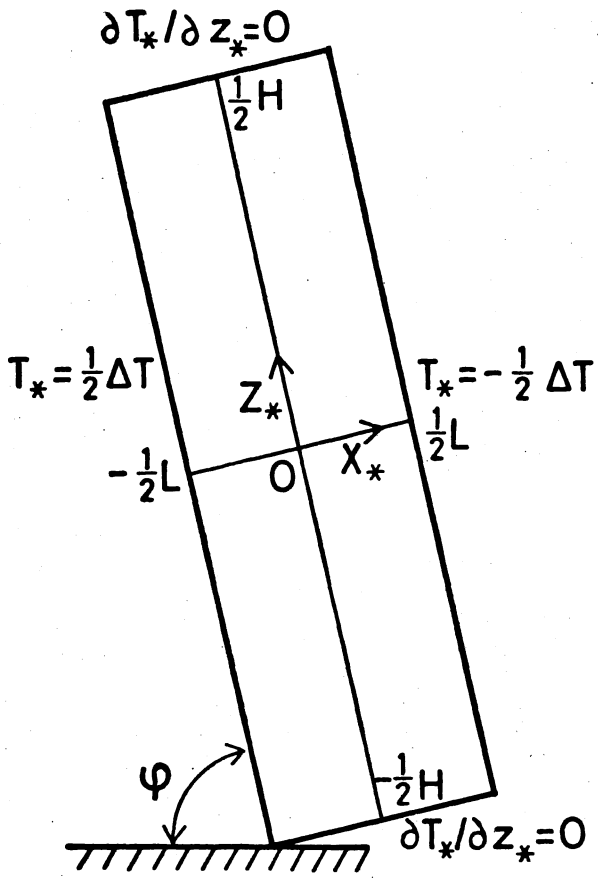

Figure 1

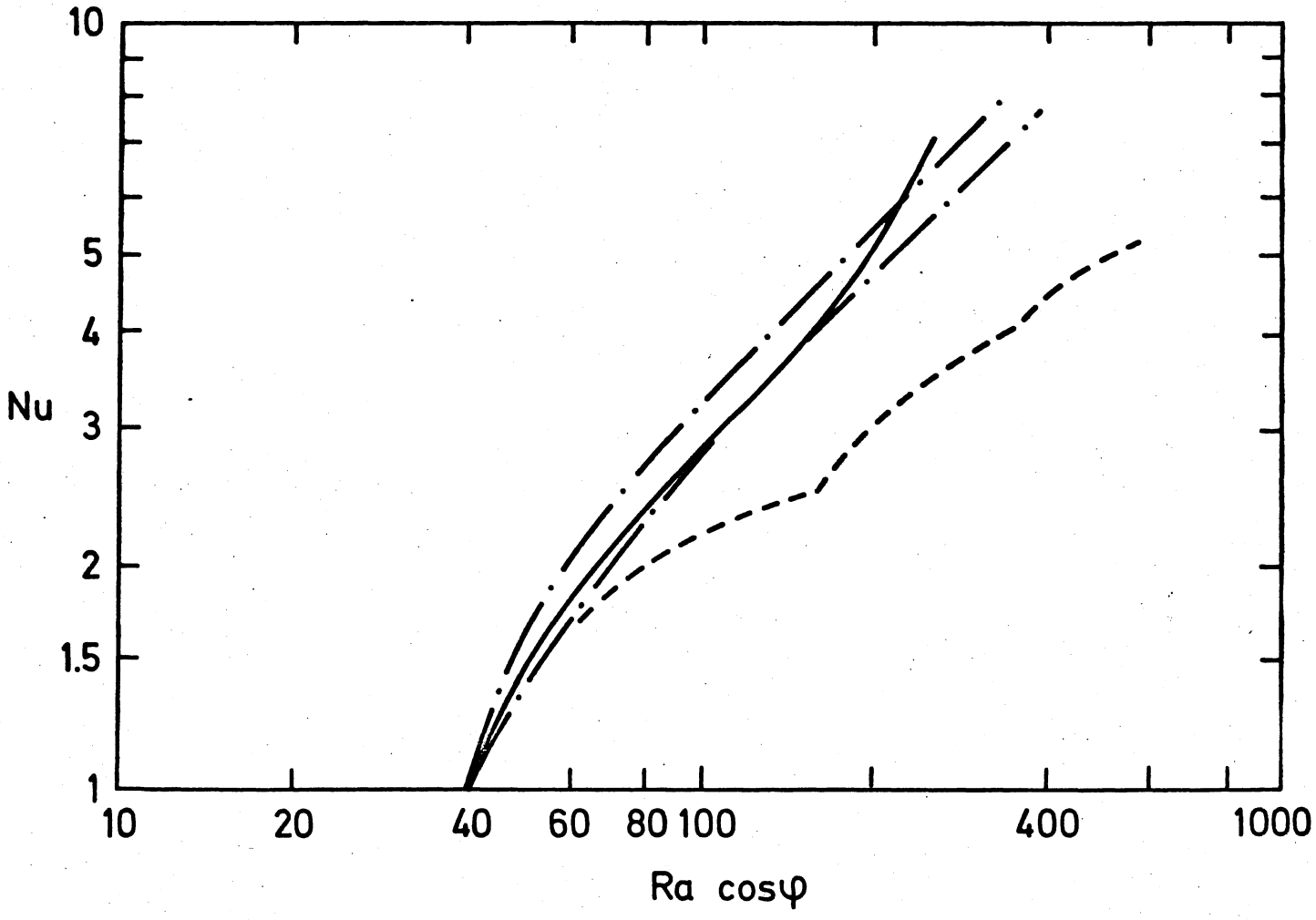

Figure 2

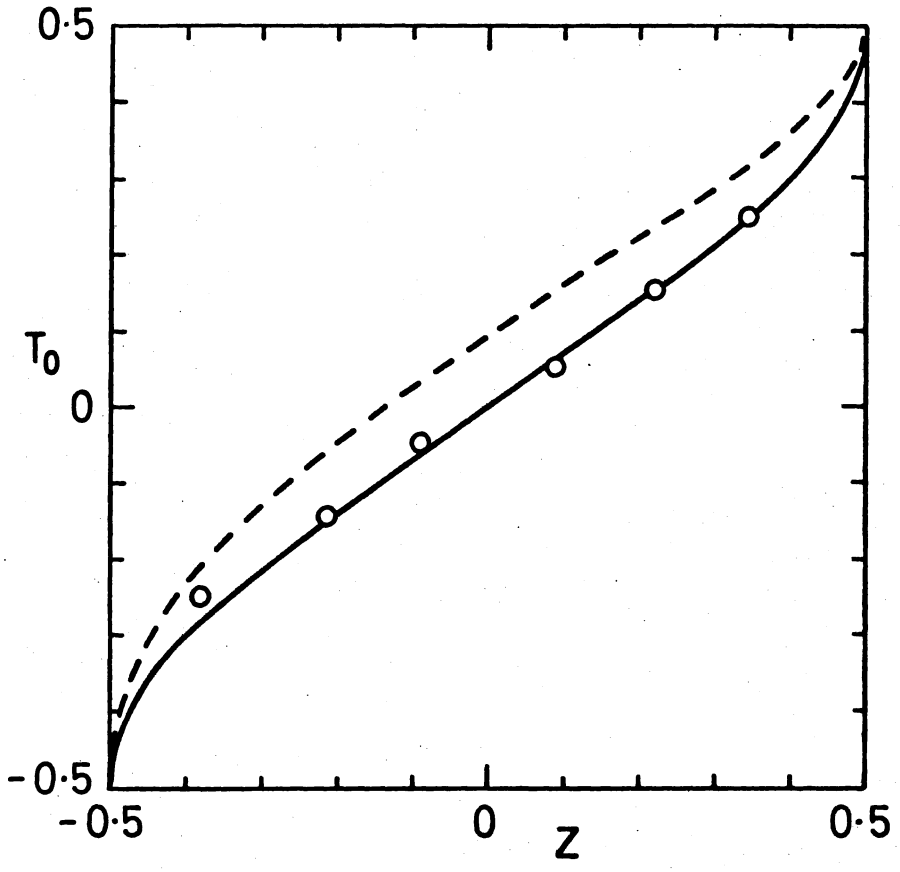

Figure 3

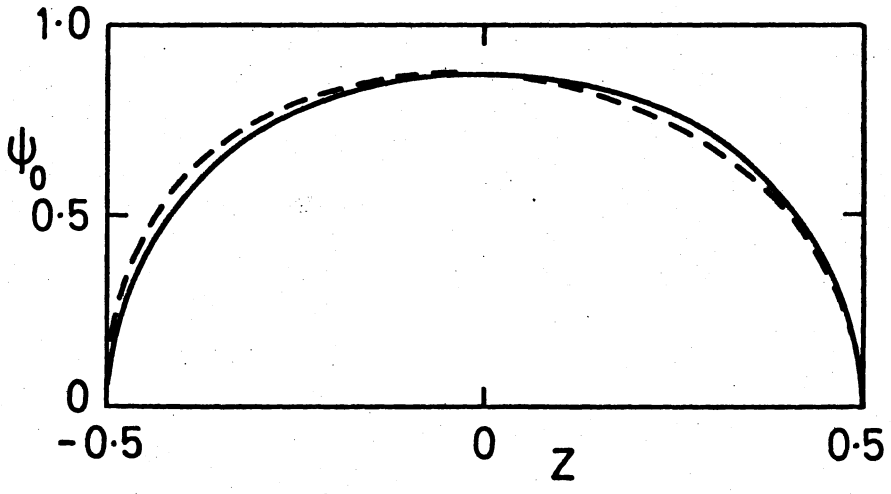

Figure 4

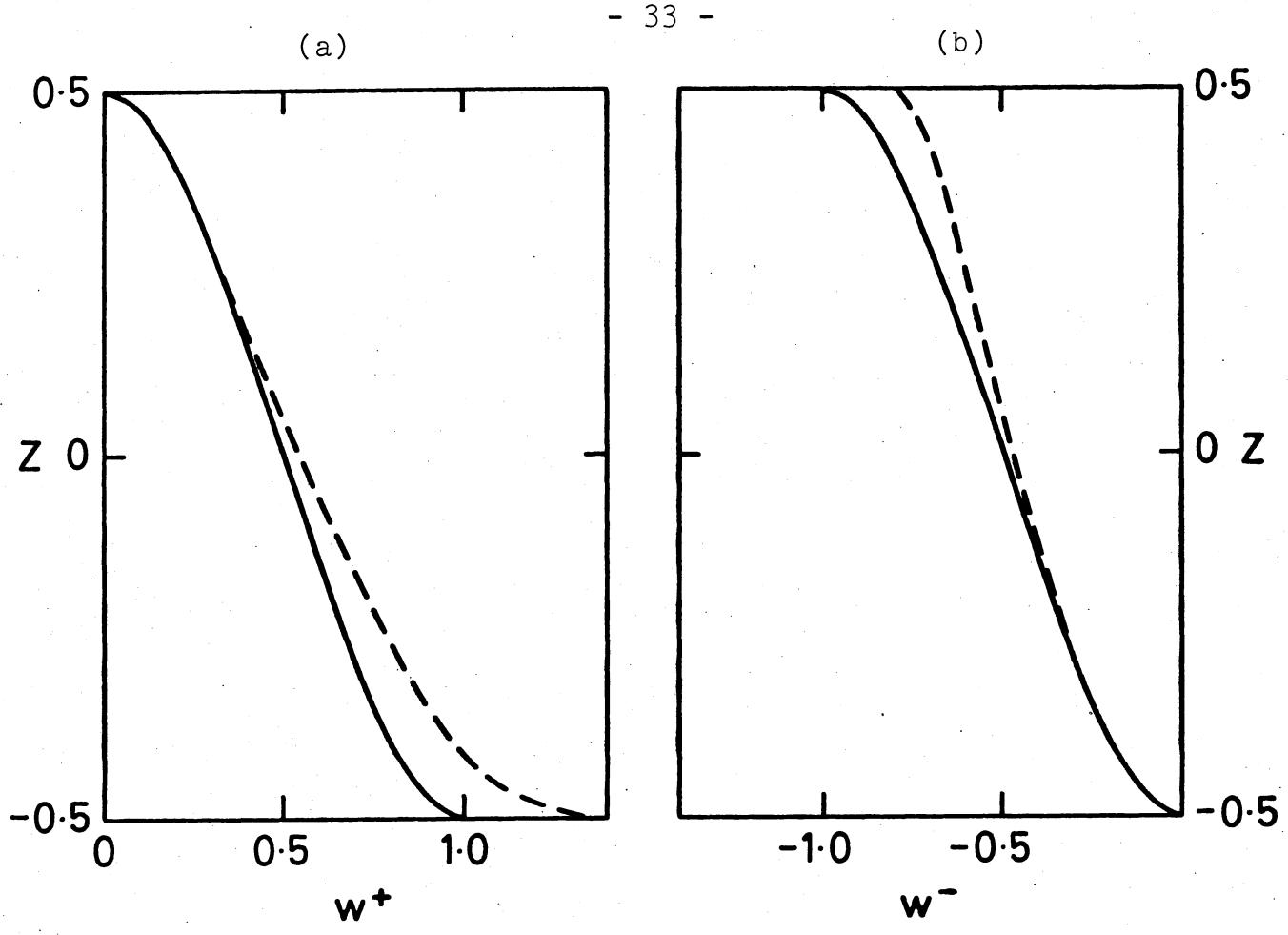

Figure 5

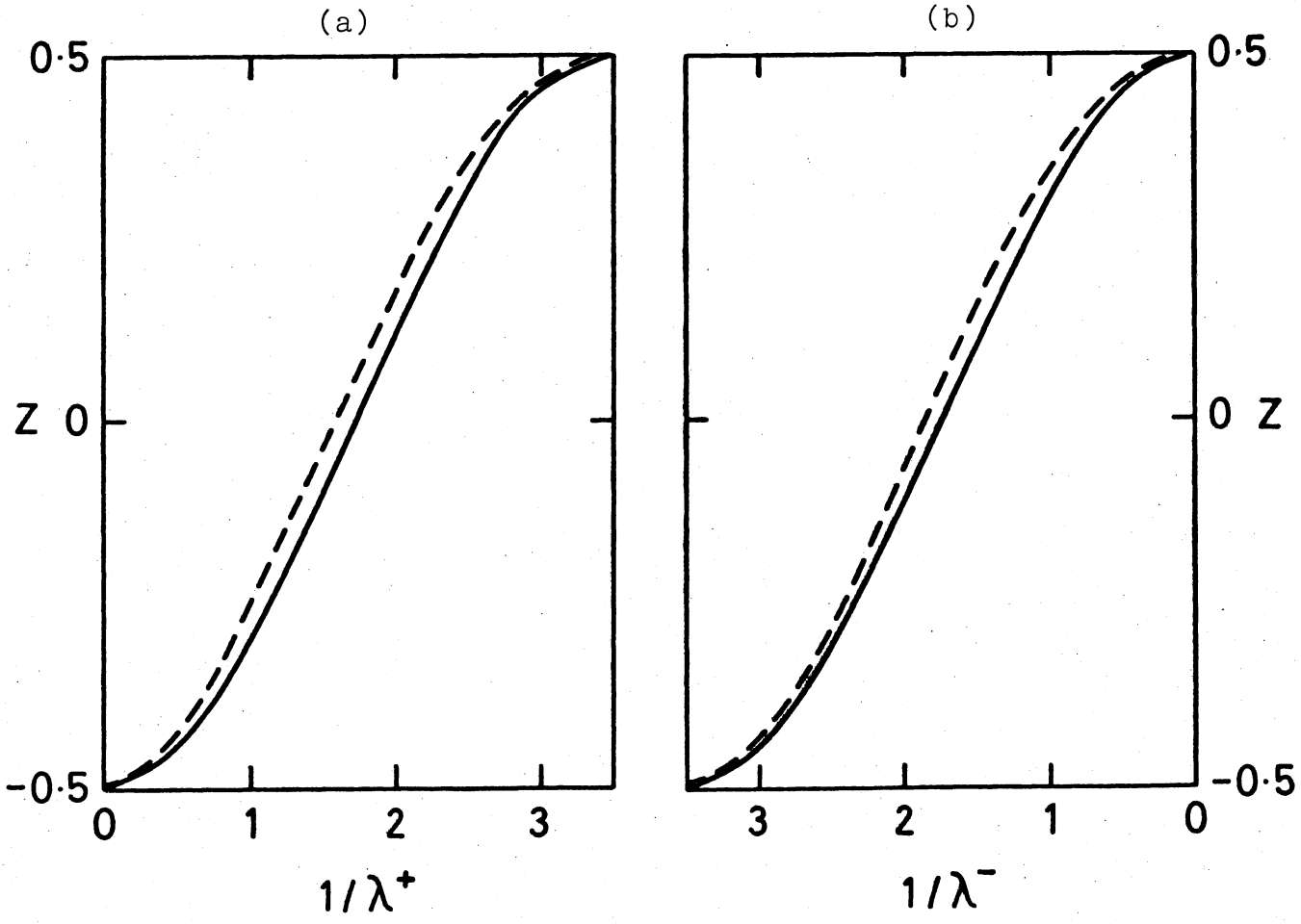

Figure 6

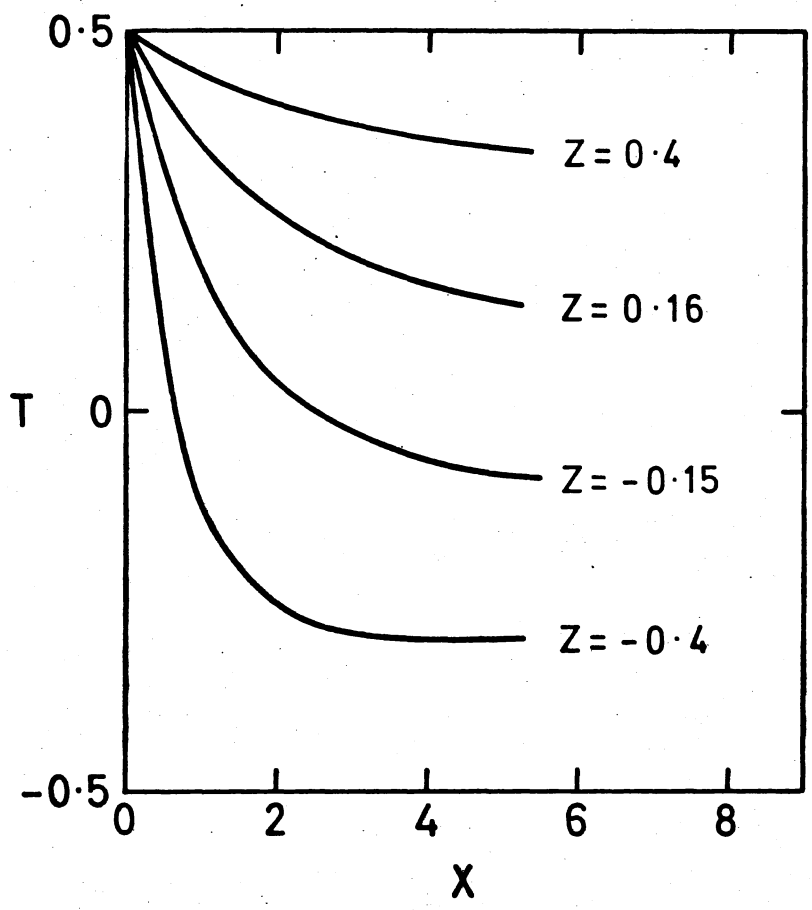

Figure 7